J Neurophysiol 103: 3287–3301, 2010.
First published March 31, 2010; doi:10.1152/jn.00024.2010.

Nociceptive Processing by Anterior Cingulate Pyramidal Neurons

Bai-Chuang Shyu,[1] Robert W. Sikes,[2] Leslie J. Vogt,[3,4] and Brent A. Vogt[3,4]

[1]*Institute of Biomedical Sciences, Academia Sinica, Taipei, Taiwan, Republic of China;* [2]*Department of Physical Therapy, Northeastern University, Boston, Massachusetts;* [3]*Cingulum NeuroSciences Institute, Manlius, New York; and* [4]*State University of New York Upstate Medical University, Syracuse, New York*

Submitted 12 January 2010; accepted in final form 24 March 2010

Shyu B-C, Sikes RW, Vogt LJ, Vogt BA. Nociceptive processing by anterior cingulate pyramidal neurons. *J Neurophysiol* 103: 3287–3301, 2010. First published March 31, 2010; doi:10.1152/jn.00024.2010. Although the cingulate cortex is frequently activated in acute human pain studies, postsynaptic responses are not known nor are links between nociceptive afferents, neuronal responses, and outputs to other structures. Intracellular potentials were recorded from neurobiotin-injected, pyramidal neurons in anterior cingulate area 24b following noxious stimulation of the sciatic nerve in anesthetized rabbits. Layer IIIc pyramids had extensive and horizontally oriented basal dendrites in layer IIIc where nociceptive afferents terminate. They had the longest excitatory postsynaptic potentials (EPSPs; 545 ms) that were modulated with hyperpolarizing currents. Pyramids in layer V had an intermediate tuft of oblique apical dendrites in layer IIIc that were 150–350 μm from somata in layer Va and 351–550 μm in layer Vb. Although average EPSP durations were short in layers II–IIIab (222 ± 31), Va (267 ± 65), and Vb (159 ± 31), there were five neurons in layers IIIab–Va that had EPSP durations lasting >300 ms (548 ± 63 ms). Neurons in layers IIIc, Va, and Vb had the highest amplitude EPSPs (6.25, 6.84 ± 0.58, and 6.4 ± 0.47 mV, respectively), whereas those in layers II–IIIab were 5 ± 0.56 mV. Nociceptive responses in layer Vb were complex and some had initial inhibitory postsynaptic potentials with shorter-duration EPSPs. Layers II–IIIab had dye-coupled pyramids and EPSPs in these layers had short durations (167 ± 33 ms) compared with those in layers IIIc–Va (487 ± 28 ms). In conclusion there are two populations of anterior cingulate cortex pyramids with EPSPs of significantly different durations, although their dendritic morphologies do not predict EPSP duration. Short-duration EPSPs are thalamic-mediated, nociceptive responses lasting ≤200 ms. Longer, "integrative" EPSPs are >350 ms and are likely modulated by intracortical axon collateral discharges. These findings suggest that links between nociception and projections to cortical and motor systems are instantaneous because nociceptive responses are generated directly by pyramidal projection neurons in all layers.

INTRODUCTION

Human imaging consistently reports acute nociceptive responses in cingulate cortex (Derbyshire 2000; Peyron et al. 2000; Vogt 2005). Although most localize to midcingulate cortex, nociceptive responses in rat and rabbit are usually in the anterior cingulate cortex (ACC; Hsu et al. 1997; Sikes and Vogt 1992; Sikes et al. 2008). Moreover, there are no innocuous responses that are not associated with nociceptive responses in the same cingulate neurons; that is to say, all neurons are either nociceptive-specific or wide-dynamic range neurons (in the works cited; Yamamura et al. 1996). Given the prominent role of ACC in pain perception (Iwata et al. 2005), anticipation of pain (Koyama et al. 1998), fear conditioning (Tang et al. 2005), and avoidance behaviors (Gabriel 1993; Pastoriza et al. 1996), it is to be expected that nociceptive discharges in ACC differ from those in the somatosensory cortex. Kuo and Yen (2005) compared noxious responses in both regions and observed neurons in ACC were less frequently activated and had a longer latency with onset as late as 700 ms and lasting for 2 s.

Nothing is known about the intracingulate mechanisms by which nociceptive information is transduced in ACC. Only one intracellular-labeling study of ACC nociceptive pyramids is available (Yamamura et al. 1996) and it showed that nociceptive-specific neurons have a wider intracortical axonal projection than that of wide-dynamic range neurons. Since all neurons were in layer V in this latter study and postsynaptic responses were not considered, nothing is yet known of nociceptive neurons in superficial layers or postsynaptic responses in any layers. Finally, studies of ACC nociception usually fail to report the cytoarchitectural layers in which responses occur because they rely on rat atlases that do not identify layers or differentiate ACC from midcingulate cortex (Vogt et al. 2004). In view of the findings in human studies, this is an important issue to address in experimental animals where such information is available.

The ACC nociceptive signal arises in thalamus, as shown with lidocaine block (Sikes and Vogt 1992), lesion (Yang et al. 2006), electrical stimulation of the thalamus (Hsu and Shyu 1997; Hsu et al. 2000), and a high correlation between midline, mediodorsal and intralaminar nuclei (MITN), and ACC nociceptive responses (Lee et al. 2007). Surprisingly, links between the laminar terminations of these inputs and postsynaptic pyramidal neuron outputs have not been explored. Nociceptive neurons are in the MITN (Casey 1966; Dong et al. 1978) and they have cingulate projections as discussed in detail in the DISCUSSION. A study of projections to the cingulate premotor areas, for example, showed intracingulate differences with the rostral cingulate premotor cortex having two- to sevenfold more such input than that of the posterior area (Hatanaka et al. 2003). Finally, the mediodorsal (MD) nucleus projects to layer IIIc, whereas the centrolateral, ventromedial, parafascicular, and reunions nuclei project to layer Ia. No studies have attempted to link these projections to pyramidal dendrite morphology and response characteristics.

Our primary hypothesis states that differences in pyramidal excitatory postsynaptic potentials (EPSPs) are determined by how they sample nociceptive synapses in layers IIIc and Ia. Thus layer IIIc pyramids have basal dendrites embedded in the terminations of MD, whereas those in layers II–IIIab do not receive such input, directly leading to the expectation that

Address for reprint requests and other correspondence: B. A. Vogt, Cingulum NeuroSciences Institute, 4435 Stephanie Drive, Manlius, NY 13104 (E-mail: bvogt@twcny.rr.com).

EPSPs in layers IIIc and V will be longer than those in layers II–IIIab. Beyond the primary hypothesis, other issues remain: what is the amplitude, duration, and variability of excitatory and inhibitory postsynaptic potentials by layer, not just layer V? This information is critical to developing an ACC model of nociceptive processing because it is unlikely that only layer V pyramids are so engaged. How might these response properties be linked to intracortical circuits and projections to other cortical and motor systems because these will be critical substrates of cingulate nocifensive behaviors? This information will be used to consider the endpoints of ACC nociceptive processing that lead to other parts of the brain.

METHODS

Animal preparation

Adult male New Zealand rabbits (3–4 kg) were used in the present experiments. Seven animals were used to develop the intracellular labeling methods, whereas 22 were used to derive the data reported here. Uses of the experimental animals and procedures were approved by the Institutional Committee for the Humane Use of Animals at SUNY Upstate Medical University.

Animals were initially anesthetized with ketamine and xylazine (35 and 5 mg/kg, respectively, administered intramuscularly) to allow insertion of a tracheal tube. Rectal temperature was monitored and maintained at 37°C with a circulating-water heating pad. The electrocardiogram was continuously monitored and recorded (HP 78352a). Hydration was maintained by a saline drip into an ear vein and surgical wounds were treated with lidocaine (lidocaine hydrochloride jelly USP, 2%; Teva Pharmaceuticals, Akron, OH). The animal was then anesthetized for surgery with a mixture of halothane (1.5–2%) and oxygen (2 L/min). The animal's head was fixed to the stereotaxic device by attaching a stainless steel bar to the cranium with skull screws and dental acrylic. Before hardening, the dental acrylic was molded into a well that was filled with sterile saline during the experiment. To minimize pulsation, small openings, about 2 × 5 mm, were made through the bone over the target cortical area, leaving the dura intact. With bregma as reference, ACC was explored from +4.0 to +6.0 mm.

After surgery, the anesthesia level was reduced to about 0.5% or until weak withdrawal reflexes could be elicited. At this level of anesthesia, there were no spontaneous movements and noxious cutaneous stimulation produced only short-duration reflexive movements of the stimulated appendage with no coordinated movements of other limbs or any other signs of arousal. Heart rate was continuously monitored during the experiment to ensure that noxious stimulation produced no increase in heart rate. After the animal reached the experimental level of anesthesia, muscle tone and reflex movements were blocked with a single dose of a neuromuscular blocking agent (pancuronium bromide 2 mg/kg, administered intravenously) and the animal was artificially ventilated (Penlon Nuffield Ventilator Model 200 with Newton valve, Abingdon, UK). Expired CO_2 concentration was continuously monitored and maintained between 3 and 4% by regulating the end tidal volume or respiratory frequency. Since reflexes cannot be monitored during neuromuscular blockade, withdrawal reflexes were carefully assessed before injection and heart rate was continuously monitored throughout the period of paralysis, ensuring that heart rate did not change in response to noxious stimulation. This blockade was effective for about 2 h, at which time the level of anesthesia was reassessed before repeating the blockade or next penetration of microelectrode. No animals showed signs of arousal after neuromuscular blockade.

Electrical stimulation of the sciatic nerve

The sciatic nerves were exposed unilaterally and a custom-made stainless steel cuff electrode was attached to it. Biphasic electrical current (0.5 ms duration, 1 Hz) was delivered by a constant current isolator (Model A385R; World Precision Instruments, Sarasota, FL) and the anode electrode was placed about 1 cm distal to the cathode. The minimal intensity for inducing hindlimb muscle twitch is a threshold value that generates a minimal muscle twitch. Sciatic nerve stimulation (SNS) was delivered at intensities that were multiples of the threshold current value with train pulses (train duration 30–50 ms; pulse frequency, 100 Hz). The A-β fibers are excited by twofold the intensity at which muscle twitches are elicited and nociceptive A-δ and C fibers are recruited by 10- and 20-fold threshold, respectively (Chang and Shyu 2001). A supramaximal threshold of 100-fold was used to ensure maximal activation of nociceptive afferent fibers. In some instances 2-, 10-, and 50-fold threshold stimulations were used to evaluate the extent to which innocuous activation could drive ACC neurons. We were unable to activate ACC neurons with 10-fold stimulations, suggesting a primary role for C fibers in generating the nociceptive response and even 50-fold stimulations evoked only a modest response (e.g., Fig. 5). In addition, receptive field studies show that the only innocuous stimuli that activate the MITN and ACC are tap stimuli and these are characteristic for nociceptive neurons only (Casey 1966; Sikes and Vogt 1992).

The goal of data collection was to use consistent stimulation parameters to generate nociceptive responses rather than to characterize the responses as nociceptive-specific neurons during the average sampling period of 1–1.5 h per neuron. A sampling period of 1 s per sweep was used because extracellular studies document long-duration nociceptive responses that can last this length of time.

Intracellular recording and analysis

Intracellular electrodes were filled with 3 M potassium acetate and 2% neurobiotin or, in a few instances, 2% biocytin (Vector Laboratories), with impedance of 40–90 MΩ. Recordings were made using an Axoclamp 900A microelectrode amplifier (Molecular Devices, Sunnyvale, CA) with ×10 amplification. Intracellular membrane potentials were recorded in bridge mode, bridge balance was continuously monitored, and capacitance compensation was adjusted at the beginning of each electrode penetration. Neurons with at least −50 mV resting membrane potentials (V_m, RMPs) and spikes of about 45 mV in amplitude were included in data collection and analysis, although group averages by layer show a generally higher amplitude of >50 mV (Table 1). The amplified signals were digitized with an A/D converter card in an IBM-compatible computer and recorded by a Windows-based data acquisition program and analyzed with a custom MATLAB program (The MathWorks, Natick, MA).

Once stable intracellular RMPs were achieved, 7–10 repetitive SNS were applied as 0.5 ms pulses at 2 Hz. Each SNS was delivered 300 ms after sweep onset and each sweep was a 1 s sample. A series of prolonged (700 ms) hyperpolarizing (−0.2 nA, with −0.2 nA increments) or depolarizing (0.2 nA with 0.2 nA increments) pulses were applied concurrently with the SNS during the 1 s sampling period with the current pulses delayed 100 ms from the initiation of the sweep and ended at 800 ms. In most cells, SNS was repeated after the polarization testing of the cells. Thus about 40 SNS were delivered and, on average, 10 electrode penetrations were attempted in each animal and no more than 400 SNS were delivered in each animal. The intensity of 100-fold threshold SNS was applied in most of the neurons with a stable RMP, whereas 10-, 20-, or 50-fold threshold were also tested in some neurons. The SNS-evoked PSPs with or without evoked action potentials were the main criteria for the nociceptive response, as shown in Table 1, and occurred for an average probability for each laminar group in ≥70% of samples.

Since the SNS tetanus lasted 20 ms, it was usually difficult to determine the exact onset of PSPs. As shown in Fig. 3, for example,

TABLE 1. *Summary of neuron properties*

Layer	Soma Size, μm^2	RMP, mV	R_{in}, MΩ	EPSP Amplitude, mV/Duration, ms*	PSP** Probability	Spike Amplitude, mV	Spike Mode
II–IIIab							
XT1/II	200, 241	−55	25	4/280	0.8	45	Single
FT9/II	399, 265	−65	29	7/170†	0.9	49	Mixed
YT3/IIIab	132	−66	14	5.5/180	0.7	56	Mixed
TT5/IIIab	175	−52	20	3.5/190	0.8	50	Single
BBT1/IIIab	188, 161	−55	45	6/160	0.8	58	Single
FT6/IIIab	NR	−66	30	4/350‡	1.0	44	Single
Mean ± SE	220 ± 29.6	−60 ± 2.7	27 ± 4.3	5 ± 0.56/222 ± 31	0.83 ± 0.4	50 ± 2.3	
IIIc							
FT3	248	−62	17	6.5/440‡	0.8	45	Mixed
BBT9	170	−50	45	6/650‡	0.6	42	Mixed
Va							
LT4	423	−52	23	10/145	0.9	62	Single
GT11	411	−75	20	7/160	1.0	67	Single
VT9	234	−52	60	6/230	0.9	59	Single
ST9	289	−60	30	4.5/180	0.9	44	Single
HT9	451	−62	28	8.2/210	0.6	72	Single
ST10	NR	−55	45	7/160	0.9	55	Single
XT4 (15)	341	−60	40	7.5/650‡	0.8	49	Single
RT8 (16)	368	−55	27	4.2/650‡	0.6	50	Single
LT6	246	−59	25	6.5/190	0.9	48	Single
RT6	626	−70	24	5.5/90	0.9	56	Single
Mean ± SE	377 ± 43	−60 ± 2.3	32 ± 3.7	6.84 ± 0.58/267 ± 65	0.84 ± 0.4	56 ± 2.8	
Vb							
RT9	187	−68	30	6.25/200	1.0	65	Single
MT3	281	−53	36	IPSP/200	1.0	43	Burst
MT4	363	−61	73§	5.5/220	0.7	44	Burst
HT8	186	−62	35	6/80	1.0	63	(PSP only)
ST3	426	−58	22	8/210	0.8	43	Mixed
ST5	171	−58	35	6/88	0.8	49	Single
Mean ± SE	268 ± 37	−60 ± 1.5	37 ± 2.57	6.39 ± 0.47/159 ± 31	0.88 ± 0.5	51 ± 4.2	

NR, not recovered; **PSP Probability: proportion evoked PSPs in *experiments* 1 and 4; †*experiment* 1, but *experiment* 4 initial IPSP; ‡EPSPs >300 ms duration; §with outlier removed, 32 ± 2.6 MW; Boxplot of EPSP durations:

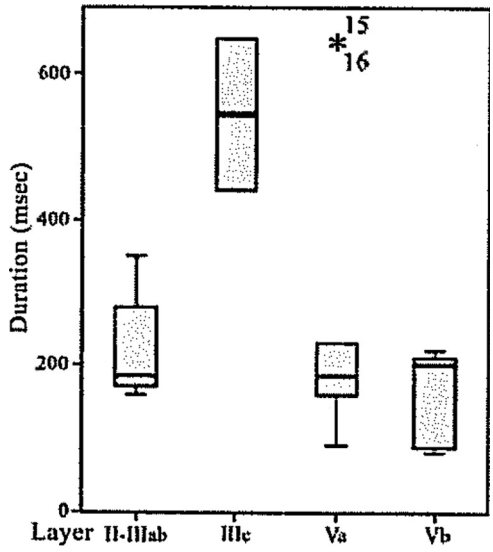

where the response is enlarged by twofold, there is an extremely short delay before the EPSPs are apparent. Since the response could have been initiated by the earlier stimuli in the tetanus, we cannot determine which part of the EPSP was associated with each SNS pulse and do not attempt to report response latencies.

Spike threshold, defined as the membrane potential corresponding to the slope break point, was expressed as the mean membrane potential at which spontaneous action potentials were triggered. In cells that did not exhibit spontaneous firing, the threshold was determined for the first spike evoked by a depolarizing intracellular current pulse. EPSP duration was measured as the time needed by the membrane potential to rise from the half-maximum EPSP membrane potential to returning to the half-maximum potential. To assess the input resistance, the slope was determined from a current–voltage plot constructed with a series of voltage responses during hyperpolarizing current pulses. Evoked voltage responses were averaged from 5 to 10

responses. The RMP was calculated by subtraction of the tip potential occurring when the microelectrode was withdrawn from the neuron.

Intracellular labeling and immunohistochemical methods

Intracellularly recorded cells were usually injected with neurobiotin using 2 nA depolarizing pulses delivered with 300 ms at a 50% duty cycle for ≥10 min. In a few early studies biocytin labeling was accomplished with 2 nA negative current injected with a duration of 500 ms and at a 50% duty cycle for 10 min. Recording electrodes were carefully withdrawn in the end of current injection and allowed at least one additional hour before brain fixation. At the end of the recording session, the rabbit was deeply anesthetized with pentobarbital (40 mg/kg, administered intraperitoneally) and perfused with 4% paraformaldehyde. The brain was postfixed in 4% paraformaldehyde for 2–3 days, soaked in 10% and 20% sucrose for 3 days, and then placed in 30% sucrose until the brain sank in solution. Blocks with the injected neurons were cut in 10 series of 40-μm-thick coronal sections using a Hacker-Bright cryostat and washed in phosphate-buffered saline (PBS). One series of sections was stained with thionin (0.05%, 3.7% sodium acetate, 3.5% glacial acetic acid, pH 4.5) for 3 min. All other sections were reacted with avidin-biotin complex (Vector) overnight in 4°C and then washed in PBS and Tris-buffered saline two times. Sections were reacted with 0.5% diaminobenzidine, nickel ammonium sulfate, and 0.01% hydrogen peroxide for 10 min, dried, and coverslipped.

Neuron classification by size, area, and layer

Neurons were used only if they could be classified morphologically. Because one in 10 sections was stained with thionin, there were two instances of the 24 pyramidal neurons that met inclusionary criteria where the soma could not be recovered as it was in the thionin-stained section. However, apical and many basal dendrites were recovered and these two neurons were classified as pyramidal by area and layer. All neurons were photographed with a MacroFire digital camera (Optronics, Goletta, CA) at ×40, ×100, and ×600. The latter photograph was of the soma and was submitted to Bioquant software (Nashville, TN). The soma was outlined to the first branch of the apical dendrite and its area calculated in μm^2; this value was used to

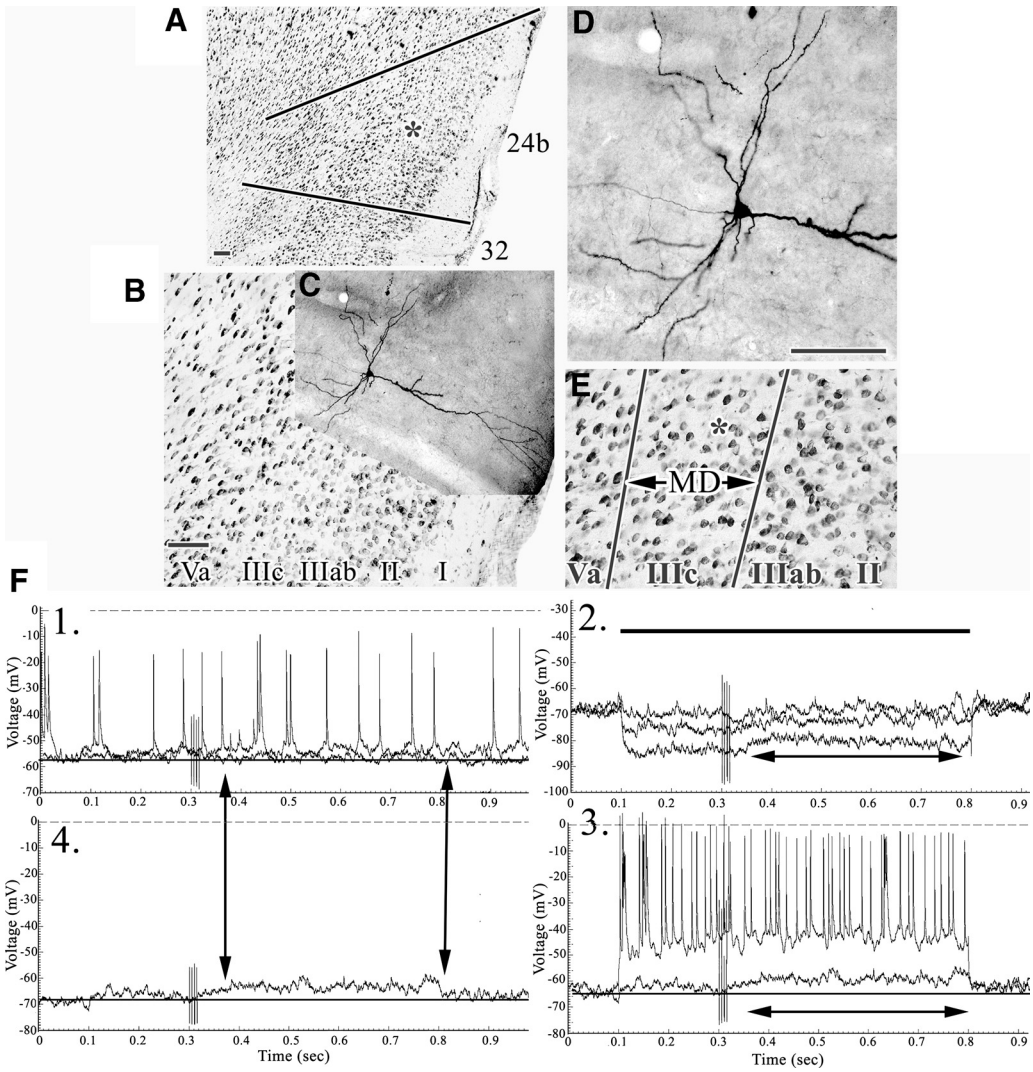

FIG. 1. *A*: layer IIIc pyramid in area 24b at the asterisk (FT3). The bottom line is the border between areas 32 and 24b, whereas the top line is between areas 24b and 8. *B*: the pyramid (*C*) is coregistered to the thionin-stained section (*B*). *D*: higher magnification of the neuron and an equivalently scaled thionin section (*E*, asterisk location of pyramid) to show the orientation of basal dendrites spanning layer IIIc and "←MD→" to emphasize the layer of thalamic termination. *F*: samples of responses to sciatic nerve stimulation (SNS) at stimulus artifact 300 ms after onset of the sampling period. Comparisons of responses in *experiments* 1 and 4 are emphasized with double arrows. The response did not appear to terminate during the 500 ms post-SNS noted with the double arrow in *experiment* 2. *Experiment* 3 also indicates a prolonged excitatory postsynaptic potential (EPSP) at a +0.2 depolarizing current pulse. Scale bars: 100 μm.

determine the size of each pyramidal neuron as medium (130–310 μm^2) or large (311–650 μm^2). The wide distribution of pyramidal neuron dendrites required that photographs from two to five sections often be used to visualize the entire dendritic tree and montages were created in Photoshop (Adobe CS2) for these large dendritic trees from as much as 240 μm of tissue.

Photographs were also taken of adjacent thionin-stained sections at ×10 and ×40 and all were imported to a separate "layer" in Photoshop. Each pair of labeled neuron and thionin-stained section was exactly coregistered to determine the area and layer in which the labeled neuron was located. All neurons were in area 24b just above or rostral to the genu of the corpus callosum and examples of rabbit area 24b cytoarchitecture have been shown in color with neuron-specific nuclear binding protein immunohistochemistry (Sikes et al. 2008) for comparison with the grayscale thionin-stained sections presented in this report. Examples of each photographic magnification are provided that show the cytoarchitecture and labeled neuron coregistered at different magnifications. In some figures, coregistration of individual neurons is presented with same-magnification, thionin-stained sections or just as the cytoarchitecture at ×40 to show differences between area 24b and area 32 ventrally. In Figs. 1 and 2, for example, area 32 is shown, which has a layer IV, whereas no layer IV is present in area 24b. Layers II and III are thicker in area 32, layer V is thinner, and layer VI is more prominent. Area 8 has very large layer Va neurons (Fig. 4*A*, asterisk) and lower densities of neurons in all layers and lacks a layer IV.

Each figure was constructed with two to five plates of essential morphology, including coregistration of labeled neurons and their

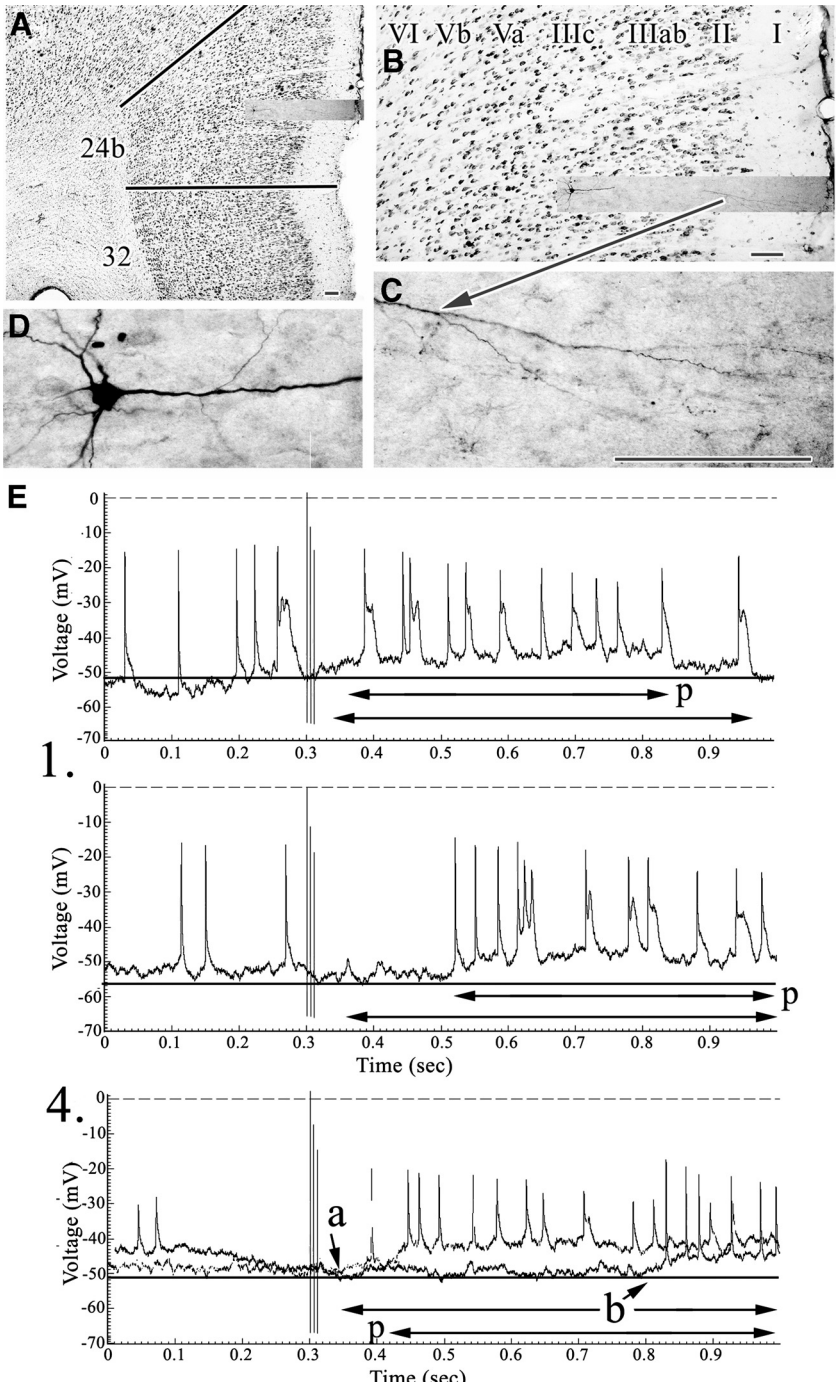

FIG. 2. *A–D*: cytoarchitecture of area 24b and coregistered pyramidal neuron (BBT9). *E*: *experiments* 1 and 4 showing durations of EPSPs. The "a" and "b" emphasize the onsets of an early and late EPSP, respectively. The double arrows labeled "p" suggest the onset and termination of maintained plateau potentials. Scale bars: 100 μm.

dendritic trees to thionin-stained sections. A series of records from four types of neurophysiological experiment are shown in the following manner. *1*) A sample of records from a series of six to eight SNS (×100). *2*) The same SNS during 700 ms hyperpolarizing pulses (two or three are shown from a sample of five/neuron). *3*) The same SNS during 700 ms depolarizing pulses of the same duration. A horizontal bar adjacent to polarity responses shows the onset and termination of these pulses. *4*) Examples of the same SNS selected from 7 to 12 stimuli that reflect the most common response patterns for each neuron. *Experiment* 4 is a second series of SNS for determining the kinetics of postsynaptic potential changes to reinforce findings in the first three experiments.

Statistical analysis of anatomical and electrophysiological measures was accomplished with SPSS (SPSS, Chicago, IL). The distribution of data was evaluated with boxplots. Parametric and nonparametric methods were used to describe and compare somal size, EPSP amplitude, and duration by cortical layer. Significance was defined as $P < 0.05$.

RESULTS

In all, 61 neurons were analyzed intracellularly; of those neurons, the morphologies of 20 were not recovered, one was in layer VI, one was in area 8, and for 15 the nociceptive responses did not reach criteria for inclusion. The following analysis is based on 24 neurons for which there was excellent morphology, stable RMPs, and SNS-evoked responses. A response was identified by postsynaptic potentials time-locked to SNS with a stable baseline on about 70% of test trials, although laminar group averages showed SNS-evoked responses >80% (Table 1). All 24 neurons were in area 24b and all had a typical pyramidal morphology with one exception—there was a fusiform pyramid in layer IIIab.

Somal area was plotted for each neuron on a continuous scale; i.e., the neurons were not placed into bins of predetermined size ranges due to the sample size. The distribution of somal sizes suggests there was a natural break point between two Gaussian distributions at 310 μm^2 and this served as the cutoff between medium and large neurons; Table 1 shows somal sizes for each neuron. Somal sizes (means ± SE) were the following by layer: II, 276 ± 43.1 μm^2 (without one outlier, 235 ± 18.8 μm^2); IIIab, 164 ± 12.7 μm^2; IIIc, 209 ± 39; Va, 377 ± 43 μm^2; Vb, 268 ± 37 μm^2. There was a

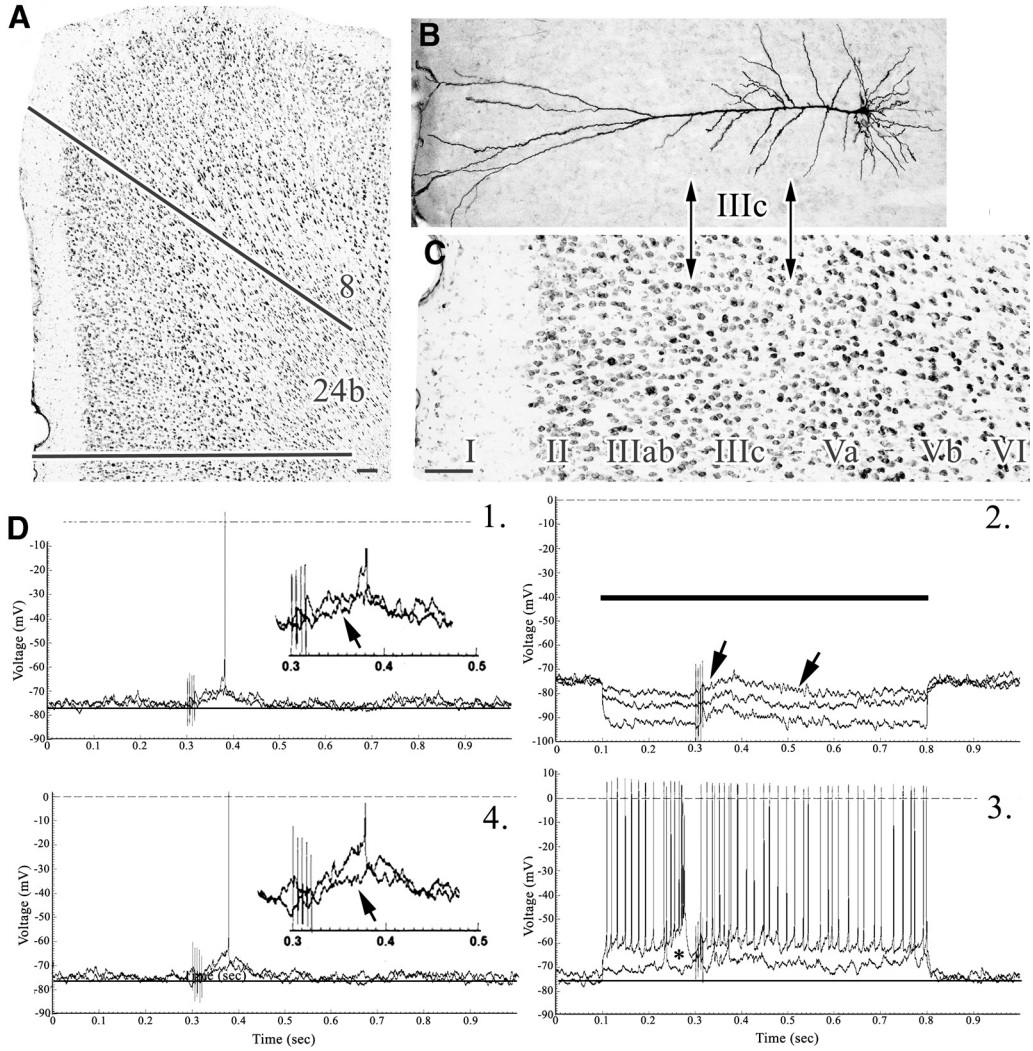

FIG. 3. *A–C*: cytoarchitecture of area 24b and coregistration of pyramid thereto (GT11). *D*: the pair of traces from *experiments* 1 and 4 show subthreshold and suprathreshold responses and include ×2 enlargements with arrows at the ramp of the EPSPs. EPSPs were modulated by hyperpolarizing currents (*2*) and the lowest amplitude depolarizing current (0.2 nA). A large potential occurs after the onset of the 0.6 nA depolarization and is associated with spike inactivation just before onset of the SNS (small asterisk). Scale bars: 100 μm.

significant difference in mean somal sizes (ANOVA, $P < 0.02$) that was confirmed with pairwise comparisons between layers IIIab and Va (Bonferroni, $P < 0.05$). Each laminar group of neurons had almost the same RMPs and input resistances (R_{in}) ($P < 0.05$; Table 1).

The variation in EPSP duration is possibly due to the different dendritic relationship that neurons in each layer have with nociceptive inputs to layer IIIc. Layer IIIc pyramids have basal dendritic skirts that ramify horizontally in layer IIIc, where mediodorsal thalamic afferents terminate (emphasized in Fig. 1*E* with "←MD→" because this is critical to the primary hypothesis), whereas those in layer Va have intermediate apical dendrites in layer IIIc. Both classes of neurons have apical tufts in layer Ia where non-MD, MITN terminate.

Overall, nociceptive EPSPs were low amplitude, with a symmetrical distribution (6.1 ± 0.31 mV). Neurons in layers IIIc, Va, and Vb had the highest amplitude EPSPs (6.25, 6.84 ± 0.58, and 6.4 ± 0.47 mV, respectively), whereas those in layers II–IIIab were 5.0 ± 0.56 mV; however, these differences were not statistically significant (ANOVA, $P > 0.05$). The EPSP durations were much less uniform. The overall distribution had a strong positive skew with five neurons having durations exceeding the upper quartile (mean 255.8; median 190 ms; SD 175.8; range 80–650 ms, the maximum recordable duration; interquartile range 120). The sample distribution differed significantly from the normal distribution (chi-square goodness of fit, $P < 0.025$) and suggests a bimodal distribution with a small population of neurons with exceptionally long EPSPs. Exclud-

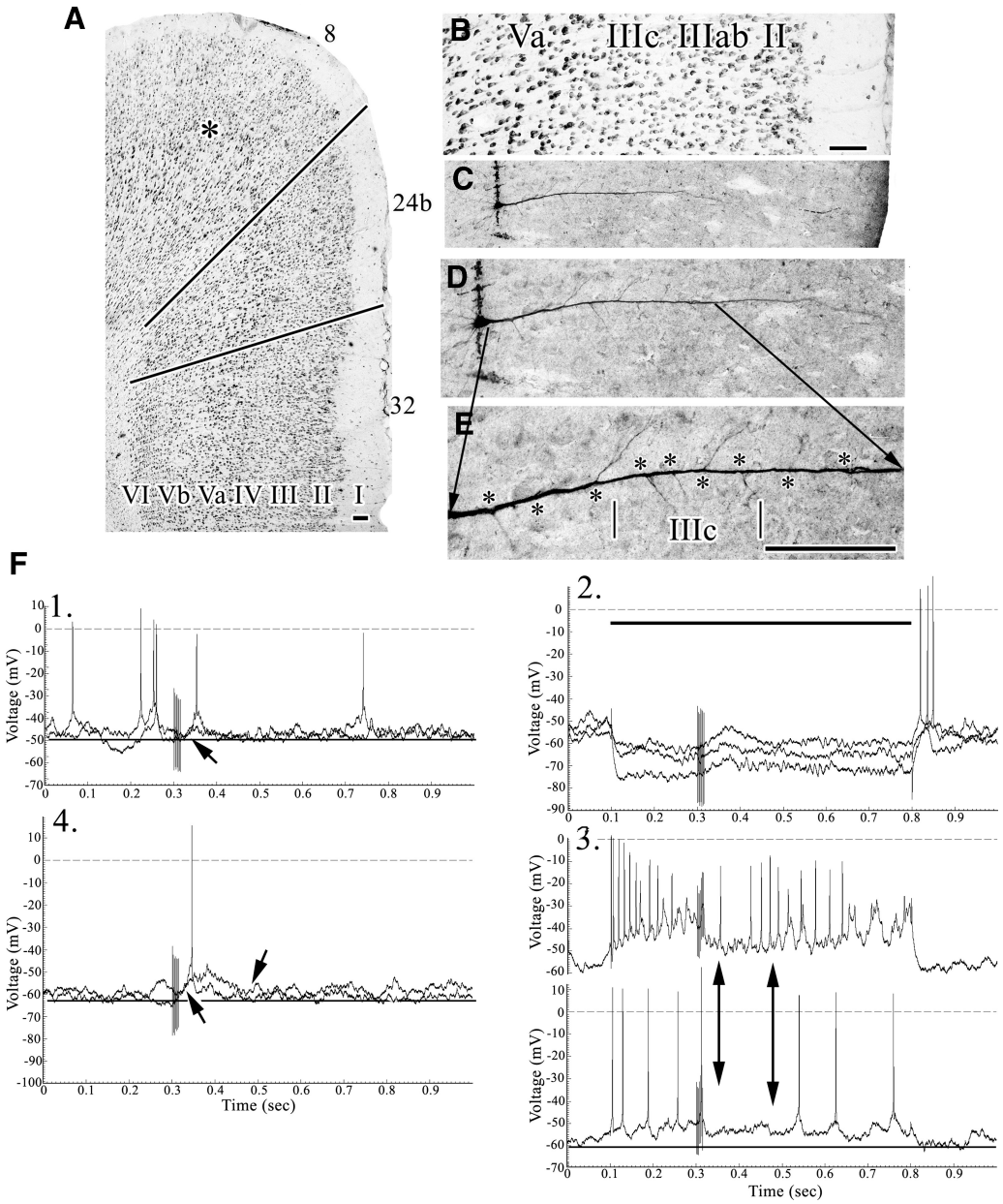

FIG. 4. *A*: structure of areas 8, 24b, and 32 with an asterisk in area 8 on layer Va for reference. *B* and *C*: coregistration of the layer Va pyramid (LT4) to area 24b layers. *D* and *E*: expanded views of the apical dendrite with asterisks opposite of each apical branch to emphasize those emitted in layer IIIc. *F*: pairs of samples in *experiments* 1 and 2 with onset of EPSPs marked and, in the latter, offset. The two double arrows in *3* emphasize a period of spike inactivation during the post-SNS period. Scale bars: 100 μm.

ing these long-duration responses, layers II–IIIab had the greatest durations (196 ± 21.6) followed by Va (176 ± 15.2), and the layer Vb durations were shortest (159.6 ± 31.0), which may be partially due to overt and underlying inhibitory postsynaptic potential (IPSP) activity, as discussed in the following text. The differences between the short-duration EPSPs, however, did not differ significantly by layer (ANOVA, $P > 0.05$). As shown in Table 1, the 5 long-duration EPSPs (‡‡) were observed in all layers (4 of 12 in layers IIIc and Va and 1 of 12 in layers II–IIIab) except Vb and both neurons in layer IIIc had long-duration EPSPs (440 and 650 ms), although an expanded sample may show some with shorter-duration responses in layer IIIc. The distribution of durations by layer is shown in a boxplot in Table 1. The difference in proportions of short- and long-duration EPSPs between these layers was not statistically significant (Fisher's Exact Test, $P = 0.158$) and these data do not support our primary hypothesis that neurons with longer EPSPs have a preferential distribution of dendrites in layer IIIc.

Layer IIIc and Va pyramidal neurons

The dendritic trees of neurons in these two layers have extensive arbors in layer IIIc to sample nociceptive synapses. Figures 1 and 2 are of layer IIIc pyramids and they show angling of basal dendrites parallel to the pial surface to maximally sample layer IIIc inputs from MD. Figures 3 and 4 are of layer Va pyramids with substantial apical branches in layers Va–IIIab (Fig. 4*E*, asterisks), including many in layer IIIc that could enhance nociceptive responsivity. Given the somal proximity of both dendritic arbors, this ensures robust nociceptive transmission from layer IIIc.

The irregular-bursting neuron in Fig. 1*F1* had evoked EPSPs to SNS that were either below or just above discharge threshold, whereas no spikes were evoked during *experiment* 4. The EPSP amplitude was maximal at 6.5 mV and their duration was about 430 ms. Hyperpolarizing current (−0.6 nA; Fig. 1*F2*) further uncovered this EPSP, which was likely generated close to the soma due to termination of MD afferents in layer IIIc (Fig. 1*E*). Measured in this manner, its duration was about 440 ms and the enhanced EPSP had not terminated by the end of the current pulse. Finally, subthreshold depolarization of the neuron with +0.2 nA (Fig. 1*F3*) showed a similar duration EPSP (double arrow) and the suprathreshold stimulation generated spike trains that were nonaccommodating. Figure 2 shows an irregularly bursting pyramid with long-duration (650 ms) and low-amplitude EPSPs (*1*, 4.5 mV; *4*, 6 mV). Of particular note is *experiment* 4, where the "a" points to the early rise of the EPSP from baseline in one trial that lasted for the remainder of the sampling period, whereas the second sample ("b") shows the EPSP beginning with a very long delay of 470 ms. Long-delay responses occurred in 4 of 11 trials in *experiment* 1 and 4 of 7 trials in *experiment* 4. The sustained depolarization could reflect a plateau potential and a double arrow labeled "p" is used to indicate the onset and duration of this event.

Large layer Va pyramids have four to eight oblique apical branches in layer IIIc that sample nociceptive activity as well as an extensive apical tuft arborizing in layer I (Figs. 3 and 4). The neuron in Fig. 3 is a montage reconstructed from four sections spanning 240 μm. The SNS in Fig. 3*D*, *1* and *4* are for one subthreshold EPSP and another above threshold; the maximal amplitude of the EPSP was 7 mV. Enlargements of these responses (×2, figure *insets*) show that the EPSPs have the form of a ramp (arrows), suggesting growing voltage changes as the nociceptive response arrives in the soma that lasts for about 90 ms. Hyperpolarizing currents of −0.2, −0.6, and −0.8 nA (Fig. 3*D2*) modulated the EPSPs and they have a calculated reversal potential of about −40 mV. A subthreshold depolarization (Fig. 3*D3*) evoked small EPSPs. Higher amplitude depolarizations uncovered a burst of large, broad, and inactivating spikes (small asterisk) and depolarization-evoked responses were nonaccommodating. In view of these responses, including that to +0.2 nA, EPSP duration was about 160 ms. The pyramidal neuron in Fig. 4 had many apical branches in layers IIIab–Va and five are in layer IIIc (Fig. 4*E*, asterisks). SNS evoked a short EPSP in *experiment* 1 that increased in amplitude, to reach a maximum of 10 mV, and lengthened duration in *experiment* 4 (Fig. 4*F4*, arrows). These long-delayed EPSPs were poorly modulated by hyperpolarizing currents, suggesting a source some distance from the putative somal recording site and spike inactivation was ap-

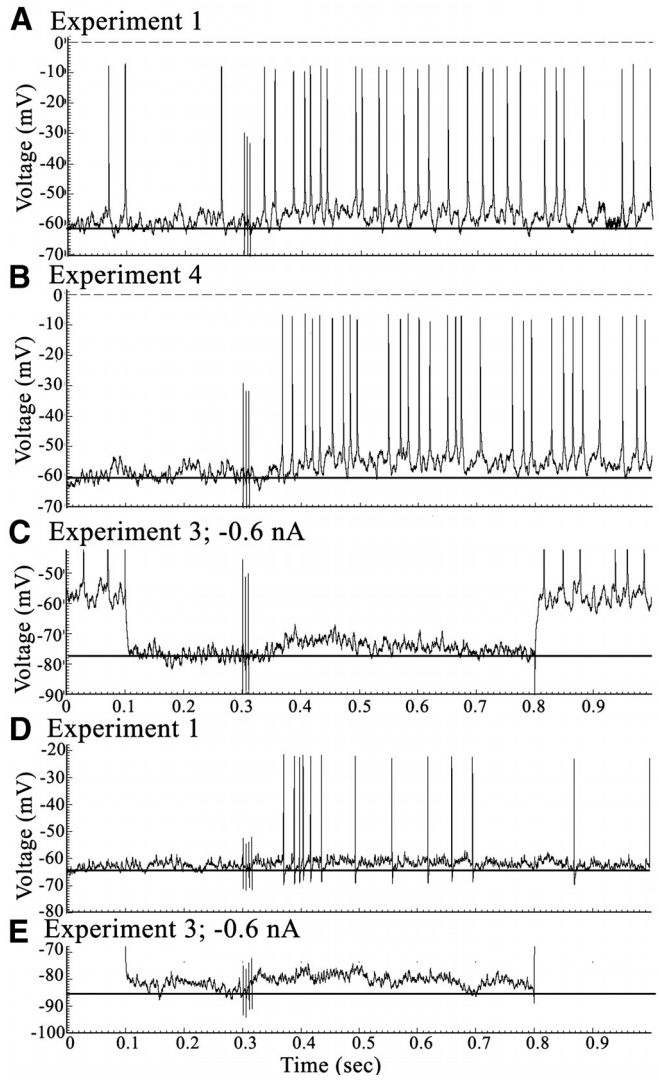

FIG. 5. Two pyramids (XT4, *A–C*; FT6, *D* and *E*) with long-duration EPSPs and verification thereof with −0.6 nA hyperpolarizing currents. Spikes in *C* were clipped to enhance figure resolution.

parent during depolarizing pulses. Of note are the higher amplitude hyperpolarizing pulses that uncover EPSPs during spike inactivation also seen during the depolarizing pulses. The four experiments together suggest the duration of the EPSP in this pyramid was 145 ms.

Although the mean, maximal EPSP amplitudes were similar for layers IIIc (6.25 mV) and Va (6.84 ± 0.58 mV), their durations were much longer in layer IIIc (545 ms) than those in Va (267 ± 65). Notice in Table 1, however, that two neurons in layer Va had very long EPSPs reaching 650 ms, the maximal length that could be determined with this sampling strategy. Figure 5 shows one of these pyramids in layer Va (Fig. 5, *A–C*) and another in layer IIIab (Fig. 5, *D* and *E*). In both instances the EPSPs were of low amplitude and spike discharges were robust following SNS and the underlying EPSP was amplified by −0.6 nA hyperpolarizing current.

Layer Vb pyramidal neurons

In spite of the fact that layer Vb pyramids have a dendritic morphology and resting membrane properties similar to those in layers IIIc–Va, their SNS responses are quite variable, as shown in Figs. 6 and 7. Figure 6 shows a pyramid with an intermediate tuft of apical dendrites in layer IIIc. Although the ×10 SNS evoked no EPSPs and the ×50 SNS generated a small and short-latency EPSP, ×100 SNS always evoked EPSPs and single spikes above threshold. The EPSPs were relatively unmodulated by hyperpolaring currents, suggesting

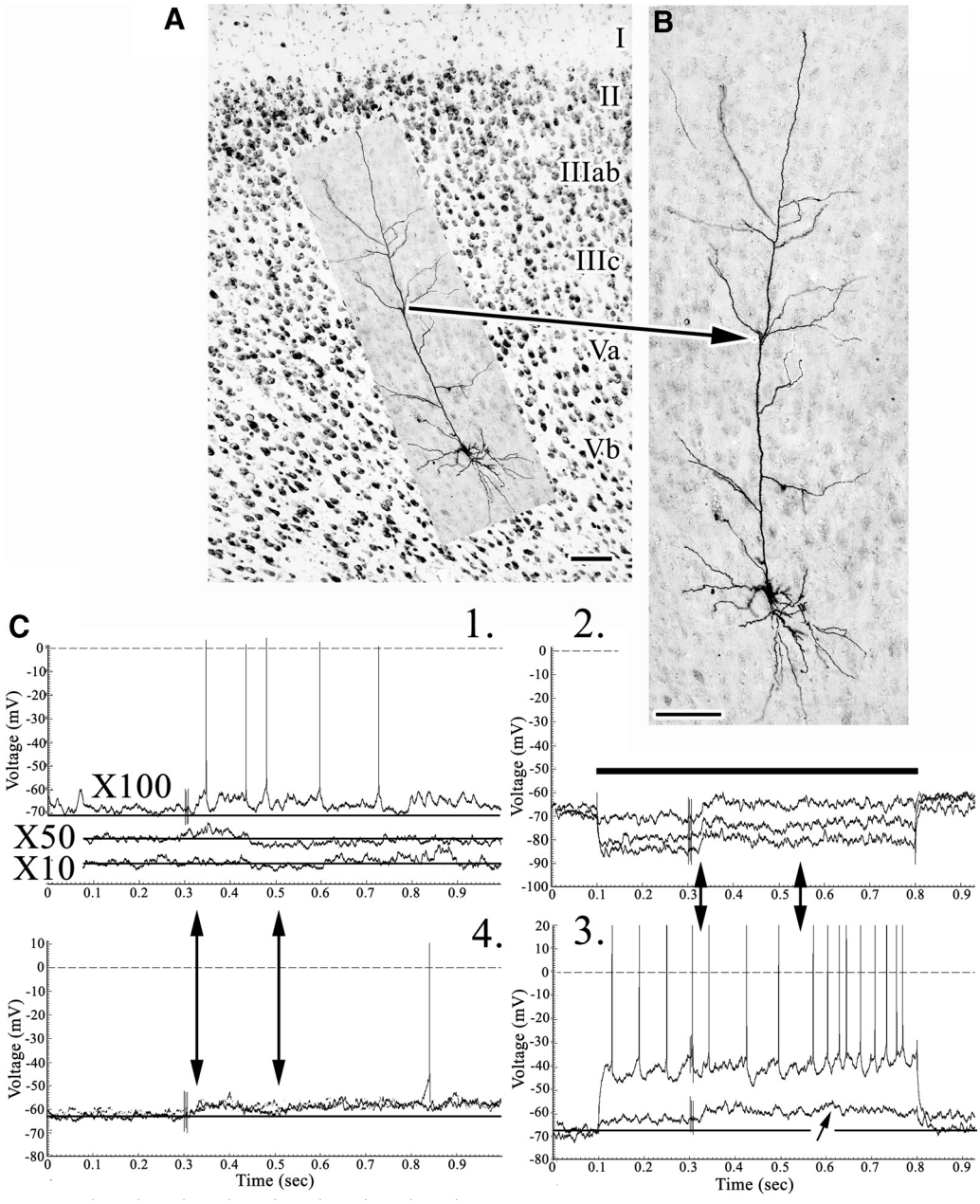

FIG. 6. *A* and *B*: layer Vb pyramid (RT9) coregistered to area 24b layers with an arrow to the intermediate apical tuft in layer IIIc. *C*: 4 experiments detailing EPSP activity following ×100 SNS. At the ×10 stimulations there was no response, whereas at the ×50 a short-duration and low-amplitude response appeared. The double vertical arrows emphasize the duration of early EPSP activity, although membrane repolarization did not occur at the highest current strength (*2*).

current sources far displaced from the soma and +0.2 nA current shows subthreshold EPSPs. EPSP parameters estimated from all four experiments suggested a maximum amplitude of 6.25 mV and duration of 200 ms.

Inhibitory activity in layer Vb pyramids occurred in two forms. One form is an overt, 250 ms IPSP preceded by an initial and brief (80 ms) EPSP (Fig. 7*A*, beginning at the asterisk in *1*). Hyperpolarizing currents greatly amplified the EPSP (*2*, asterisk) and the −0.8 nA hyperpolarization (third trace in *2*) reversed in part the IPSP, although not with the time course at baseline in *experiment* 1. Another form of inhibition occurred where IPSPs were not seen at baseline and hyperpolarizing currents were necessary to show the reversal potential during the first 200 ms at −80 mV (asterisk in Fig. 7*B2*). At baseline, this IPSP was reflected as a period of quiescence following SNS in *experiments* 1 and 4 with a similar duration (double vertical arrows).

Layers II–IIIab pyramidal neurons

Neurobiotin injections into layers II–IIIab resulted in labeling not only individual neurons but also pairs of neurons and this never occurred in layers IIIc–Vb. Four pairs of neurons were observed in layers II–IIIab (including one pair of multipolar neurons); 3 that were individually labeled in layer IIIab, and 18 neurons that were individually labeled in layers IIIc–Vb. All neurons observed in layers II–IIIab (total four pairs) were dye coupled, whereas none of the labeled neurons in deeper layers showed coupling. This difference is statistically significant (Fisher's Exact Test, $P < 0.003$). Somal sizes in each pair were almost identical: 3 largest neurons in each pair, 276 ± 63 μm^2; 3 smallest neurons in pair, 208 ± 30 μm^2.

The pyramids in Fig. 8 were very closely apposed and the arrows in Fig. 8*D* emphasize the sites of closest apposition between the apical dendrite of one and the soma of the other. Both neurons have extensive apical branching in layer I and basal dendrites throughout layer II (Fig. 8*C*, arrows). Because these neurons lean toward the layer I/II border, a circle over the thionin-stained section with asterisks emphasizes there are many such neurons in layer II. SNS generated threshold EPSPs and a −0.6 nA hyperpolarizing current uncovered an EPSP (Fig. 8*E2*).

Figure 9 shows a pair of medium-sized pyramids in layer IIIab with apical dendrites closely apposed (Fig. 9*B*, arrow). They had a low-amplitude EPSP evoked by SNS (Fig. 9*C*, *1* and *4*) that was very sensitive to hyperpolarizing currents (Fig. 9*C2*, asterisk) with an approximate reversal potential of −48 mV, suggesting the nociceptive input was close to the soma; i.e., apical tufts in layer Ia and possibly the basal dendrites extended into layer IIIc. The SNS-evoked EPSPs were not detectable during depolarizing currents and discharges did not

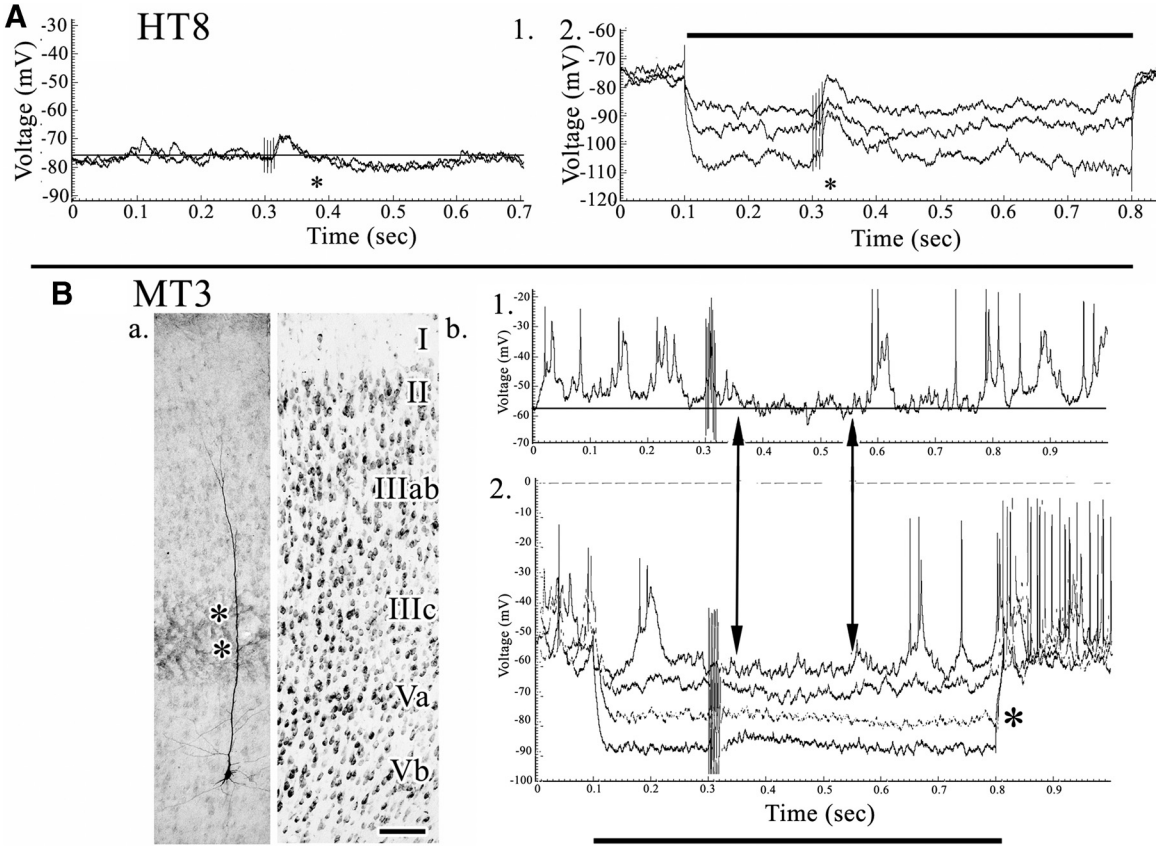

FIG. 7. Two forms of inhibitory postsynaptic potential (IPSP) activity in layer Vb. *A*: nociceptive biphasic response in pyramid HT8. *1*: EPSP arising from the SNS artifact and terminated by an IPSP at asterisk. The short duration of onset is likely associated with the first pulse of the SNS. *2*: a large EPSP was uncovered by hyperpolarizing currents (first asterisk). *B*: bursting pyramidal neuron MT3 with an intermediate apical dendritic tuft in layer IIIc (asterisks) and interruption of SNS-evoked activity without an overt IPSP. *1*: burst-mode firing was interrupted following SNS and EPSP activity and spike inactivation was apparent. *2*: the 0.6 nA hyperpolarizing pulse occurred at the approximate reversal potential (asterisk; gray trace). Vertical pairs of arrows emphasize the period of response modulation in the post-SNS period. Scale bars: 100 μm.

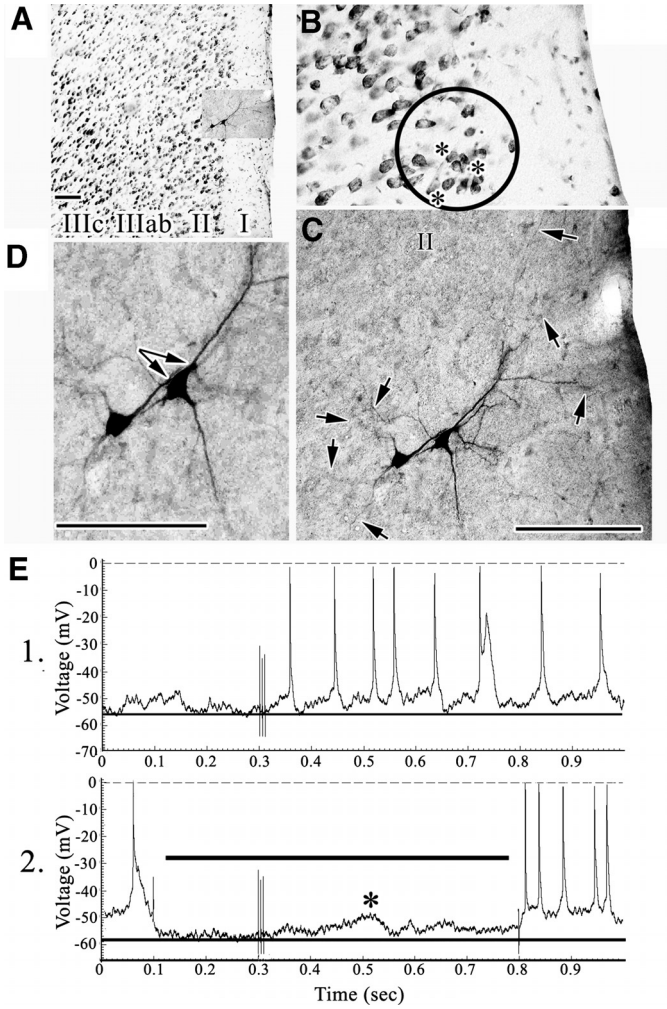

FIG. 8. *A–D*: pair of layer II pyramids (XT1). In *B* the circle emphasizes part of layer II and asterisks mark leaning neurons, whereas the arrows in *C* point to many of the basal dendrites in layer II and apical dendrites in layer I. The paired arrows in *D* show the close apposition of the apical dendrite of one neuron with the soma and apical dendrite of the other. *E*: SNS evokes regular spiking. An EPSP was uncovered by −0.2 nA current (*2*, asterisk) with a delay associated with SNS-evoked spike discharges in *1*. Scale bars: 100 μm.

accommodate (Fig. 9*C3*). The EPSP is estimated to be 160 ms in duration for this pair of neurons.

DISCUSSION

Key findings of these studies and physiological/anatomical correlations are summarized in Fig. 10. The duration of EPSPs in ACC neurons consists of a predominant population with short durations and a smaller population of neurons with significantly longer durations. A critical feature of nociceptive pyramids in layers IIIc and V is that they have extensive dendritic arbors in layer IIIc, where MD terminates (Vogt et al. 1981). Since our sampling strategy selected nociceptive neurons and passed by nonnociceptive neurons, the latter neurons may not have such apical branches and are minimally or nonresponsive to SNS. Most of the ACC pyramids shown by Yamamura et al. (1996) had this dendritic compartment, whereas layer V pyramids in sensorimotor cortex do not; i.e., apical dendrites extend through layer III without such branching (Chagnac-Amitai et al. 1990; Schwindt and Crill 1997).

Our primary hypothesis predicted that pyramids with the most extensive dendritic arbors in layer IIIc would have the longest-duration EPSPs because this is where MD terminates (Fig. 10, *1*). This hypothesis was rejected because only 4 of 12 neurons in layers IIIc–V had long-duration EPSPs, whereas all 12 had layer IIIc dendritic branches, and this was not significantly greater than the distribution in layers II–IIIab. Indeed, although two layer Va pyramids had 650 ms duration EPSPs, the average duration of all other neurons in this layer was only 171 ± 15 ms. Also, layer Vb had neurons with intermediate apical dendritic tufts in layer IIIc (Fig. 10*E*), yet the average duration of all EPSPs was only 159 ± 31. Thus there are two populations of ACC pyramids with EPSPs of significantly different durations, but their dendritic morphologies do not predict EPSP duration. For this reason, we hypothesize that the long-duration responses, which are likely very important for corticocortical integration, are mediated by excitatory, intracortical axon collaterals of nociceptive pyramids and this feature is part of the ACC nociceptive processing model discussed in the following text.

One of the key findings to emerge from these studies is that there are at least two forms of nociceptive activity and each is likely mediated by different mechanisms; Fig. 10 shows examples of short- and long-duration EPSPs. The first form of activity is a thalamic-mediated, nociceptive response that lasts for $\lesssim$200 ms and the second is a longer one that is usually $\gtrsim$350 ms. Thalamic afferents must contribute to the initial responses of both populations of EPSPs. Figure 10(*1*) shows two classes of thalamic projections to superficial layers in area 24b. Ablation of MD and staining for axon degeneration is on the left, where most input terminates in layer IIIc, and a minor amount in layer Ia with axons of passage in deep layers. In contrast, layer Ia receives most input from the midline and intralaminar nuclei; reunions (Re) are shown with autoradiographic localization of labeled terminals (Herkenham 1978); however, other MITN project to layer I, including the ventromedial nucleus (Herkenham 1979; Minciacchi et al. 1986), centrolateral nucleus (Cunningham and Levay 1986), and parafascicular nucleus (Royce and Mourey 1985; Royce et al. 1989). Each of these nuclei contains nociceptive neurons (Casey 1966; Dong et al. 1978).

The second nociceptive phase is a long-duration response that occurs in a subpopulation of layer IIIc–Va pyramids and may be subserved by excitatory, intracortical axon collaterals of nociceptive pyramids. This long-duration activity may be critical for integrative processes following the primary, thalamic-mediated, nociceptive response. Yamamura et al. (1996) showed that nociceptive-specific ACC neurons have a wider intracortical distribution than that of wide-dynamic range neurons. Although the model in Fig. 10 cannot differentiate these specific differences, a series of pyramidal intrinsic axon collaterals are shown that would enhance longer-latency discharges in nociceptive neurons [Fig. 10(*2*), ascending arrows and asterisk]. Also, it has been recently shown in the mouse that superficial layer pyramids have synaptic connections with adjacent pyramids (Wu et al. 2009) and this is included in the model from layer IIIab. Finally, inhibitory activity in layer Vb pyramids, in particular, sculpts EPSPs by significantly shortening their duration (159 ± 31 ms) and this may have a profound impact on nociceptive signals transmitted to other parts of the brain. Thus long-duration, excitatory, nociceptive

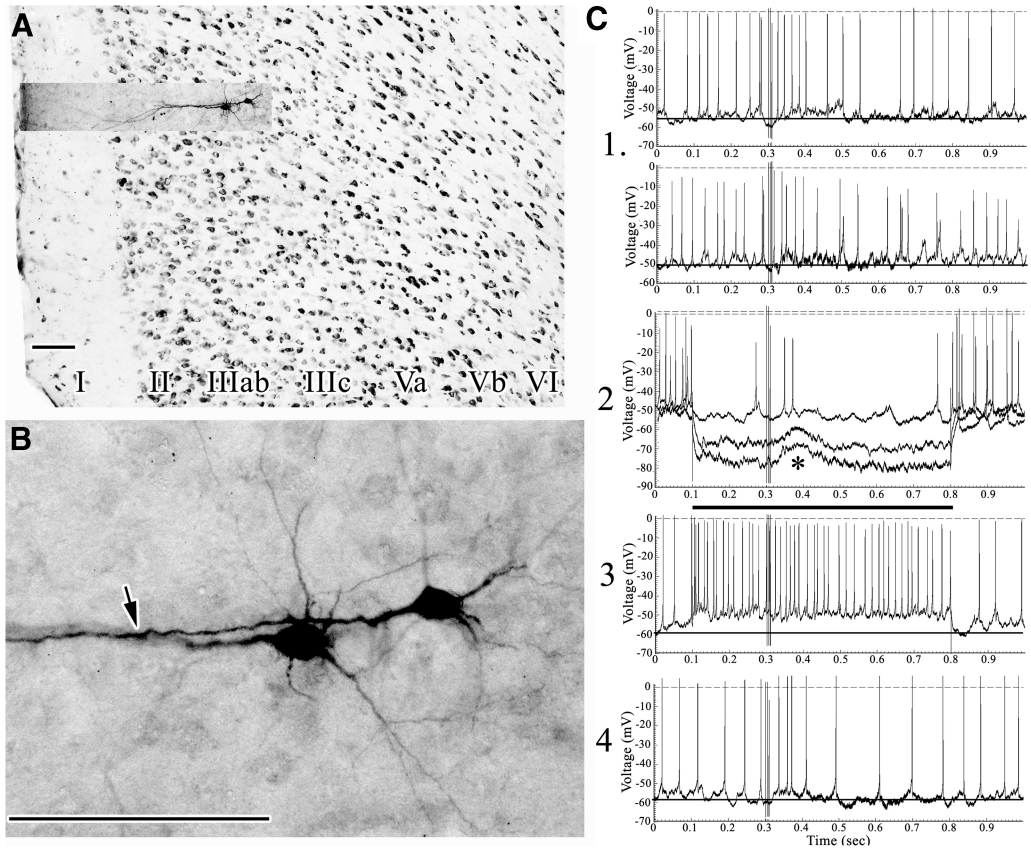

FIG. 9. *A* and *B*: layer IIIab pyramids (BBT1). Arrow points to a close apposition of the primary apical dendrites. *C*: early EPSPs (<170 ms) occur in *experiments* 1 and 4 and they were responsive to hyperpolarizing current pulses (*2*, asterisk). Depolarizing currents generally evoked single spiking with no adaptation (*3*). The EPSP-evoked spiking following SNS was prominent in *4*. Scale bars: 100 μm.

responses are likely supported by intracingulate axon collateral discharges, whereas the short-duration responses are either entirely generated in the thalamus or modulated by inhibitory intracortical circuits.

Integrative processes in cingulate cortex with other cortical activity are necessary for extending neuronal activity for pain perception (Iwata et al. 2005), anticipation of pain (Koyama et al. 1998), fear conditioning (Tang et al. 2005), and avoidance/pain behaviors (Gabriel 1993; Pastoriza et al. 1996). We emphasize long-duration EPSPs as subserving such integrative processes and Ca^{2+}-mediated plateaus may be critical for long-duration, nociceptive input with other cortical activity such as interactions of area 24b with retrosplenial area 30 and visual area 18 (Vogt et al. 1986). Long-lasting, dendritic, Ca^{2+}-dependent plateaus may be a critical part of synaptic integration distal to somata and they were explored in layer V pyramids at different distances from the soma in vitro (Oakley et al. 2001). These investigators concluded that linear increases in action potentials occurred until they saturated and plateaus were not generated in somal and proximal dendrites. A minimal duration of plateaus is about 600 ms, burst firing cannot be generated during the plateau (Schwindt and Crill 1999), and activation begins at around −45 mV. Since glutamate evokes Ca^{2+}-mediated plateaus from basal dendrites and the thalamocingulate afferents are glutamatergic and terminate on distal dendrites, these findings are relevant to ACC. Milojkovic et al. (2007) evoked Ca^{2+}-mediated plateaus with glutamate that were 0.5–2 s in duration and associated with a brief reduction of dendritic excitability; we observed spike inactivation during plateau potentials in layer IIIc and layer Vb pyramids. Proximal plateaus may have prevented the same events arising in distally placed sites. Thus processing during the integrative, nociceptive phase shown in Fig. 10 likely depends on long-duration, Ca^{2+}-mediated events that are supported by intracingulate axon collateral discharges.

The endpoint of cingulate nociception is not simple sensation, although it might contribute to it, but prediction of nociceptor stimulation and guidance of nocifensive behaviors. This perspective has been recently codified into the Cingulate Premotor Pain model that identifies three tiers of cingulate organization in primates, beginning with the primary nociceptive response and leading to autonomic and skeletomotor outputs (Vogt and Sikes 2009). The observations of the present study speak directly to links between nociceptive and output systems, given that each layer of pyramids in rabbit and rat has different projection targets and these projections are summarized in Fig. 10(*3*). Indeed, the link between nociceptive activity and motor output appears to be instantaneous in both species because it occurs directly on output neurons.

As a rule, corticocortical connections are made by pyramids in layer III and to a lesser extent in layer Va (Vogt et al. 1986). These projections of area 24b are substantial to area 30 (previously termed area 29d) and visual area 18 and are shown in Fig. 10(*3*). Motor system projections originate from layer Vb to the spinal cord (Miller 1987) and from layer Va to the striatum, ventral tegmental area, and periaqueductal gray (Gabbott et al.

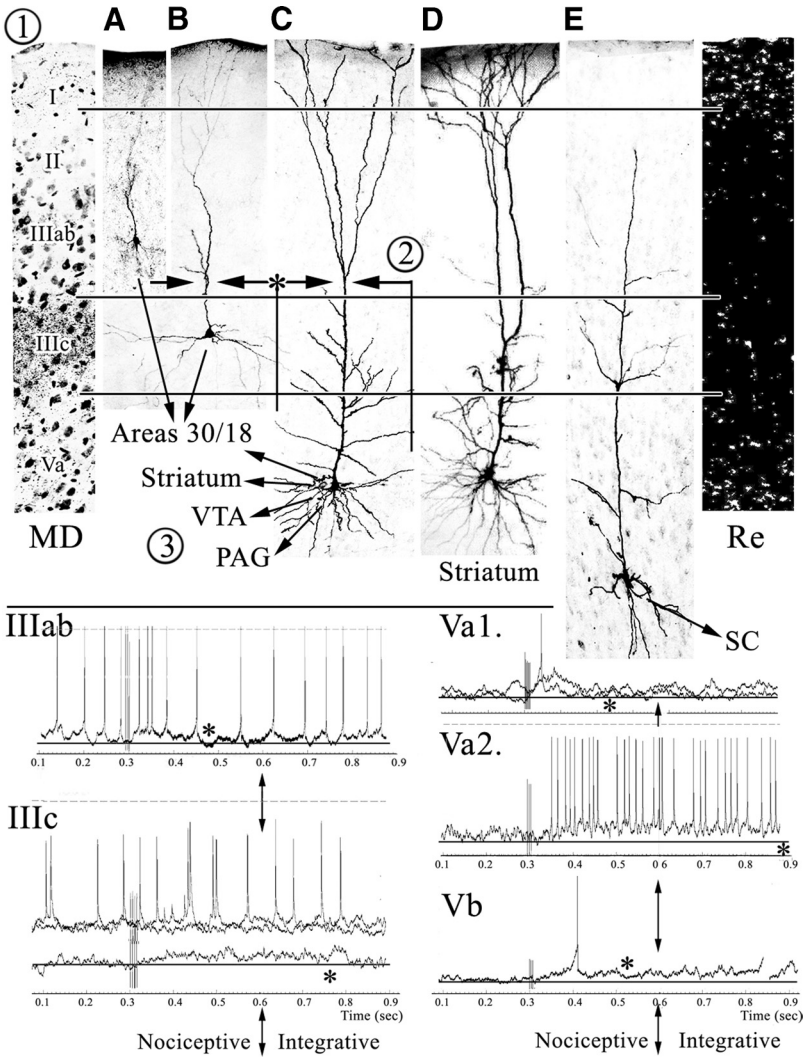

FIG. 10. Overview of physiological/anatomical correlates. *1*: thalamic [MD and Reuniens-Re-projections from Vogt et al. (1981) and Herkenham (1978), respectively], nociceptive neurons *A–C* and *E* from the present study and a cingulostriatal neuron from Zheng and Wilson (2001; *D*). *2*: intrinsic axon collaterals of superficial pyramids from Wu et al. (2009) and deep lying pyramids. *3*: projections of pyramids to cortical (areas 30 and 18) and motor (striatum, ventral tegmental area [VTA], periaqueductal gray [PAG], and spinal cord [SC]) structures. Examples of short- and long-duration EPSPs recorded in the present study are from layers IIIab, IIIc, Va, and Vb. The asterisks identify the termination of each EPSP and the vertical arrows note the junction between short- and long-duration responses, which is approximately at 300 ms; i.e., between the nociceptive and integrative phases of the SNS-evoked responses.

2005; Geisler et al. 2007; Sesack et al. 1989). The cingulostriatal neuron in Fig. 10*D* was filled extracellularly with neurobiotin by Zheng and Wilson (2002) and is coregistered in the figure to emphasize that it has a morphology similar to that of nociceptive, layer Va pyramids. Given these projections and laminar characteristics of nociceptive neurons, we propose that long-duration EPSPs might be associated with corticocortical projection neurons. The many other projections of layers Va and Vb with short EPSPs suggest that the nociceptive signal may engage motor system projection neurons and is characterized by a tighter link to the noxious stimulus than is the case for corticocortical projection neurons. Thus the long-duration integration phase is likely an intrinsic cortical event associated with corticocortical projections and associative processing, whereas the phasic, nociceptive, thalamic-mediated activity is associated with brain stem projections to motor systems.

The present observations of dye-coupled pairs of pyramidal neurons in layers II–IIIab constitute only the second such demonstration for neocortical pyramids. Dye coupling mediated by gap junctions is well known for nonpyramids (Connors and Long 2004; Gibson et al. 2005). Electrotonic coupling among multipolar bursting neurons was reported in neocortex (Blatow et al. 2003), among parvalbumin-containing fast-spiking neurons (Kawaguchi and Kubota 1997), and calretinin-expressing neurons (Caputi et al. 2009). Mercer et al. (1996) observed coupling between pairs of rat, neocortical pyramids with dual intracellular recordings. These pyramids were either adjacent in layers III–V or between layer III and layer V neurons. Based on the latency to spikelet onset, brief, nonfluctuating amplitudes and insensitivity to changes in membrane potentials, they concluded these are not chemical synapses. Although they were not able to identify gap junctions electron microscopically, the appositions were always at very proximal soma/dendritic membranes that were consistent with interactions between the electrically coupled neurons. Our pairs of pyramids are not explained by penetrating multiple neurons, given that stable recordings from one neuron were documented and multiple recordings were not made following a completed study. The distances and orientations of the labeled somata nullifies that they were sequentially penetrated in a single probe perpendicular to the layers of area 24b. Neuron pairs were usually between neurons of a similar type and size in the same layers (no interlayer dye coupling was observed) and there were points of very close apposition between somata and apical dendrites, as was true of the pairs reported by Mercer et al. (1996), that provide for the possibility of gap junction formation. Although recoding from layers II–IIIab in ACC is difficult, given the proximity of the midsagittal sinus, more

studies are needed to verify gap junctions and electrotonic coupling and their functional significance.

In conclusion, nociceptive responses of pyramidal neurons were more complex than anticipated and identifying possible links between dendritic morphology and nocireceptive layers requires a more detailed anatomical approach than has been generally used in the past. It was not possible, however, to predict the SNS-evoked EPSP responses based on specializations in dendritic morphology. Short-duration (<200 ms) EPSPs are directly driven by thalamic afferents from the MITN, including MD, and the long-duration responses raise the question of intracortical processing by axon collaterals of nociceptive pyramidal neurons and generation of Ca^{2+}-mediated plateaus that provide a mechanism for long-term events mediated by ACC such as pain perception, anticipation, and avoidance. The link between nociceptive activation and pyramidal neuron discharges into cortical, sensory, and motor systems is immediate and we now hypothesize that long-duration responses are associated mainly with corticocortical projection neurons, whereas those projecting to motor systems are of shorter duration and link the noxious stimulus more tightly with motor control. Finally, the presence of dye-coupled pyramidal neurons raises new questions about nociceptive processing in relation to the amygdala and other outputs of layers II–IIIab.

GRANTS

This research was supported by National Science Council and Academia Sinica grants to B.-C. Shyu and National Institute of Neurological Disorders and Stroke Grant R01-NS-44222 to B. A. Vogt.

DISCLOSURES

No conflicts of interest are declared by the authors.

REFERENCES

Blatow M, Rozov A, Katona I, Hormuzdi SG, Meyer AH, Whittington MA, Caputi A, Monyer H. A novel network of multipolar bursting interneurons generates theta frequency oscillations in neocortex. *Neuron* 38: 805–817, 2003.

Caputi A, Rozov A, Blatow M, Monyer H. Two calretinin-positive gabaergic cell types in layer 2/3 of the mouse neocortex provide different forms of inhibition. *Cereb Cortex* 19: 1345–1359, 2009.

Casey KL. Unit analysis of nociceptive mechanisms in the thalamus of the awake squirrel monkey. *J Neurophysiol* 29: 727–750, 1966.

Chang C, Shyu B-C. A fMRI study of brain activations during non-noxious and noxious electrical stimulation of the sciatic nerve of rats. *Brain Res* 897: 71–81, 2001.

Changnac-Amital Y, Luhmann HJ, Prince DA. Burst generating and regular spiking layer 5 pyramidal neurons of rat neocortex have different morphological features. *J Comp Neurol* 296: 598–613, 1990.

Connors BW, Long MA. Electrical synapses in the mammalian brain. *Ann Rev Neurosci* 27: 393–418, 2004.

Cunningham ET, Levay S. Laminar and synaptic organization of the projection from the thalamic nucleus centralis to primary visual cortex in the cat. *J Comp Neurol* 254: 65–77, 1986.

Derbyshire SWG. Exploring the pain neuromatrix. *Curr Rev Pain* 6: 467–477, 2000.

Dong WK, Ryu H, Wagman IH. Nociceptive responses of neurons in medial thalamus and their relationship to spinothalamic pathways. *J Neurophysiol* 41: 1592–1613, 1978.

Gabbott PLA, Warner TA, Jays PRL, Salway P, Busby SJ. Prefrontal cortex in the rat: projections to subcortical autonomic, motor, and limbic centers. *J Comp Neurol* 492: 145–177, 2005.

Gabriel M. Discriminative avoidance learning: a model system. In: *Neurobiology of Cingulate Cortex and Limbic Thalamus*, edited by Vogt BA, Gabriel M. Boston, MA: Burkhäuser, 1993, p. 478–523.

Geisler S, Derst C, Veh RW, Zahm DS. Glutamatergic afferents of the ventral tegmental area in the rat. *J Neurosci* 27: 5730–5743, 2007.

Gibson JR, Beierlein M, Connors BW. Functional properties of electrical synapses between inhibitory interneurons of neocortical layer 4. *J Neurophysiol* 93: 467–480, 2005.

Hatanaka N, Tokuno H, Hamada I, Inase M, Ito Y, Imanishi M, Hasegawa N, Akazawa T, Nambu A, Takada M. Thalamocortical and intracortical connections of monkey cingulate motor areas. *J Comp Neurol* 462: 121–138, 2003.

Herkenham M. The connections of the nucleus reunions thalami: evidence for a direct thalamo-hippocampal pathway in the rat. *J Comp Neurol* 177: 589–610, 1978.

Herkenham M. The afferent and efferent connections of the ventromedial thalamic nucleus in the rat. *J Comp Neurol* 183: 487–518, 1979.

Hsu M-M, Kung J-C, Shyu B-C. Evoked responses of the anterior cingulate cortex to stimulation of the medial thalamus. *Chin J Physiol* 43: 81–89, 2000.

Hsu M-M, Shyu B-C. Electrophysiological study of the connection between medial thalamus and anterior cingulate cortex in the rat. *Neuroreport* 8: 2701–2707, 1997.

Iwata K, Kamo H, Ogawa A, Tsuboi Y, Noma N, Mitsubishi Y, Taira M, Koshikawa N, Kitagawa K. Anterior cingulate cortical neuronal activity during perception of noxious thermal stimuli in monkeys. *J Neurophysiol* 94: 1980–1991, 2005.

Kawaguchi Y, Kubota Y. GABAergic cell subtypes and their synaptic connections in rat frontal cortex. *Cereb Cortex* 7: 476–486, 1997.

Koyama T, Tanaka YZ, Mikami A. Nociceptive neurons in the macaque anterior cingulate cortex activate during anticipation of pain. *Neuroreport* 9: 2663–2667, 1998.

Kuo C-C, Yen C-T. Comparison of anterior cingulate and primary somatosensory responses to noxious laser-heat stimuli in conscious behaving rats. *J Neurophysiol* 94: 1825–1836, 2005.

Lee C-M, Chang W-C, Chang K-B, Shyu B-C. Synaptic organization and input-specific short-term plasticity in anterior cingulate cortical neurons with intact thalamic inputs. *Eur J Neurosci* 25: 2847–2861, 2007.

Mercer A, Bannister AP, Thomson AM. Electrical coupling between pyramidal cells in adult cortical regions. *Brain Cell Biol* 35: 13–27, 2006.

Miller MW. The origin of corticospinal projection neurons in rat. *Exp Brain Res* 67: 339–351, 1987.

Milojkovic BA, Zhou W-L, Antic SD. Voltage and calcium transients in basal dendrites of the rat prefrontal cortex. *J Physiol* 585: 447–468, 2007.

Minciacchi D, Bentivoglio M, Molinari M, Kultas-Ilinsky K, Ilinsky IA, Macchi G. Multiple cortical targets of one thalamic nucleus: the projections of the ventral medial nucleus in the cat studied with retrograde tracers. *J Comp Neurol* 252: 106–129, 1986.

Oakley JC, Schwindt PC, Crill WP. Dendritic calcium spikes in layer 5 pyramidal neurons amplify and limit transmission of ligand-gated dendritic current to soma. *J Neurophysiol* 86: 504–527, 2001.

Pastoriza LN, Morrow TJ, Casey KL. Medial frontal cortex lesions selectively attenuate the hot plate response: possible nocifensive apraxia in the rat. *Pain* 64: 11–17, 1996.

Peyron R, Laurent B, Garcia-Larrea L. Functional imaging of brain responses to pain: a review and meta-analysis. *Neurophysiol Clin* 30: 263–288, 2000.

Royce GJ, Gracco BC, Beckstead RM. Thalamocortical connections of the rostral intralaminar nuclei: an autoradiographic analysis in the cat. *J Comp Neurol* 288: 555–582, 1989.

Royce GJ, Mourey RJ. Efferent connections of the centromedian and parafascicular thalamic nuclei: an autoradiographic investigation in the cat. *J Comp Neurol* 235: 277–300, 1985.

Schwindt P, Crill W. Local and propagated action potentials evoked by glutamate iontophoresis on rat neocortical pyramidal neurons. *J Neurophysiol* 77: 2466–2483, 1997.

Schwindt P, Crill W. Mechanisms underlying burst and regular spiking evoked by dendritic depolarization in layer 5 cortical pyramidal neurons. *J Neurophysiol* 81: 1341–1354, 1999.

Sesack SR, Deutch AY, Roth RH, Bunney BS. Topographical organization of the efferent projections of the medial prefrontal cortex in the rat: an anterograde tract tracing study with *Phaseolus vulgaris* leucoagglutinin. *J Comp Neurol* 290: 213–242, 1989.

Sikes RW, Vogt BA. Nociceptive neurons in area 24 of rabbit cingulate cortex. *J Neurophysiol* 68: 1720–1732, 1992.

Sikes RW, Vogt LJ, Vogt BA. Distribution and properties of visceral nociceptive neurons in rabbit cingulate cortex. *Pain* 135: 160–174, 2008.

Tanaka E, Higashi H, Nishi S. Membrane properties of guinea pig cingulate cortical neurons in vitro. *J Neurophysiol* 65: 808–821, 1991.

Tang J, Ko S, Ding H-K, Qiu C-S, Calejesan AA, Zhuo M. Pavlovian fear memory induced by activation in the anterior cingulate cortex. *Mol Pain* 1: Article 6. 2005.

Vogt BA. Pain and emotion interactions in subregions of the cingulate gyrus. *Nat Rev Neurosci* 6: 533–545, 2005.

Vogt BA, Rosene DL, Peters A. Synaptic termination of thalamic and callosal afferents in cingulate cortex of the rat. *J Comp Neurol* 201: 265–283, 1981.

Vogt BA, Sikes RW. Cingulate nociceptive circuitry and roles in pain processing: the cingulate premotor pain model. In: *Cingulate Neurobiology and Disease*, edited by Vogt BA. Oxford, UK: Oxford Univ. Press, 2009, p. 311–338.

Vogt BA, Sikes RW, Swadlow HA, Weyand TG. Rabbit cingulate cortex: cytoarchitecture, physiological border with visual cortex, and afferent cortical connections of visual, motor, postsubicular, and intracingulate origin. *J Comp Neurol* 248: 74–94, 1986.

Vogt BA, Vogt LJ, Farber NB. Cingulate cortex and disease models. In: *The Rat Nervous System* (3rd ed.), edited by Paxinos G. New York: Elsevier Academic Press, 2004, p. 705–727.

Wu L-J, Li X, Chen T, Ren M, Zhuo M. Characterization of intracortical synaptic connections in the mouse anterior cingulate cortex using dual patch clamp recording. *Mol Brain* 2: 1–12, 2009.

Yamamura H, Iwata K, Tsuboi Y, Toda K, Kitajima K, Shimizu N, Nomura H, Hibiya J, Fujita S, Sumino R. Morphological and electrophysiological properties of ACCx nociceptive neurons in rats. *Brain Res* 735: 83–92, 1996.

Yang J-W, Shih H-C, Shyu B-C. Intracortical circuits in rat anterior cingulate cortex are activated by nociceptive inputs mediated by medial thalamus. *J Neurophysiol* 96: 3409–3422, 2006.

Zheng T, Wilson CJ. Corticostriatal combinatorics: the implications of corticostriatal axonal arborizations. *J Neurophysiol* 87: 1007–1017, 2001.